Stem Cell Research 39 (2019) 101510

Contents lists available at ScienceDirect

Stem Cell Research

journal homepage: www.elsevier.com/locate/scr

Lab Resource: Multiple Cell Lines

Generation of two human induced pluripotent stem cell (hiPSC) lines from a long QT syndrome South African founder population

Manuela Mura[a], Federica Pisano[a,b], Manuela Stefanello[a], Monia Ginevrino[c,d], Marina Boni[e], Federica Calabrò[a], Lia Crotti[f,g,h], Enza Maria Valente[c,d], Peter J. Schwartz[f], Paul A. Brink[i], Massimiliano Gnecchi[a,b,j,*]

[a] Coronary Care Unit and Laboratory of Experimental Cardiology for Cell and Molecular Therapy, Fondazione IRCCS Policlinico San Matteo, Pavia, Italy
[b] Department of Molecular Medicine, Unit of Cardiology, Università degli studi di Pavia, Pavia, Italy
[c] Department of Molecular Medicine, Unit of Genetics, University of Pavia, Pavia, Italy
[d] Neurogenetics Unit, Fondazione IRCCS Santa Lucia, Rome, Italy
[e] Laboratory of Oncohaematological Cytogenetic and Molecular Diagnostics, Division of Haematology, Fondazione IRCCS Policlinico San Matteo, Pavia, Italy
[f] Istituto Auxologico Italiano, IRCCS, Center for Cardiac Arrhythmias of Genetic Origin and Laboratory of Cardiovascular Genetics, Milan, Italy
[g] Istituto Auxologico italiano, IRCCS, Department of Cardiovascular, Neural and Metabolic Sciences, San Luca Hospital, Milan, Italy
[h] Department of Medicine and Surgery, Università Milano-Bicocca, Milan, Italy
[i] Department of Internal Medicine, University of Stellenbosch, Tygerberg, South Africa
[j] Department of Medicine, University of Cape Town, Cape Town, South Africa

ABSTRACT

We generated PSMi001-A and PSMi008-A hiPSC lines from two individuals belonging to a South African (SA) founder population in which the malignant KCNQ1-A341V mutation cosegregates with the Long QT Syndrome (LQTS) phenotype. PSMi001-A was derived from an asymptomatic KCNQ1-A341V mutation carrier, whereas PSMi008-A was derived from a healthy non-mutation carrier, heterozygous for the minor variant rs16847548 on the *NOS1AP* gene, associated with QT prolongation in the general population, and with a greater risk for cardiac arrest in the affected members of the SA founder population. The hiPSCs, generated using the Yamanaka's retroviruses, display pluripotent stem cell features and trilineage differentiation potential.

Resource utility

iPSCs and iPSC-CMs can be efficiently used to model LQTS and to test novel pharmacological therapies (Mehta et al., 2018; Gnecchi et al., 2017; Schwartz et al., 2019). PSMi001-A cell line in particular will be useful to elucidate the pathological mechanism underlying the malignant KCNQ1-A341V mutation, while the PSMi008-A line will be of help to elucidate cellular mechanisms by which variants of the *NOS1AP* gene can influence the QT interval prolongation and the arrhythmic risk.

Resource details

Founder effects, by which many individuals share a mutation identical by descent, represent a powerful tool to understand the underlying disease causing mechanisms and to predict the natural history of mutation-associated effects.

PSMi001-A and PSMi008-A cell lines were generated from two members of a SA founder population segregating a malignant KCNQ1-A341V mutation causing a severe form of LQTS type 1 (LQT1) (Brink et al., 2005).

LQTS is an autosomal dominant inherited disease which is associated with high risk of sudden cardiac death (SCD) (Brink et al., 2005). LQT1 is the most common LQTS sub-type, accounting for ~40–50% of all LQTS cases. It is caused by mutations in the *KCNQ1* gene, encoding for the α-subunit of the voltage-dependent potassium channel responsible for the delayed rectifier potassium current (I_{Ks}), one of the repolarization currents in the heart.

PSMi001-A was derived from the fibroblasts of a 53 years old woman carrying the disease-causing mutation but who never experienced cardiac symptoms. PSMi008-A was derived from a 52 years old man who is wild type (wt) for *KCNQ1* but carries the rs16847548 minor variant on the *NOS1AP* gene in heterozygosis. We have previously de-

* Corresponding author at: University of Pavia and Fondazione IRCCS Policlinico S. Matteo, Pavia, Italy.
E-mail address: m.gnecchi@unipv.it (M. Gnecchi).

https://doi.org/10.1016/j.scr.2019.101510
Received 25 February 2019; Received in revised form 6 June 2019; Accepted 22 July 2019
Available online 24 July 2019

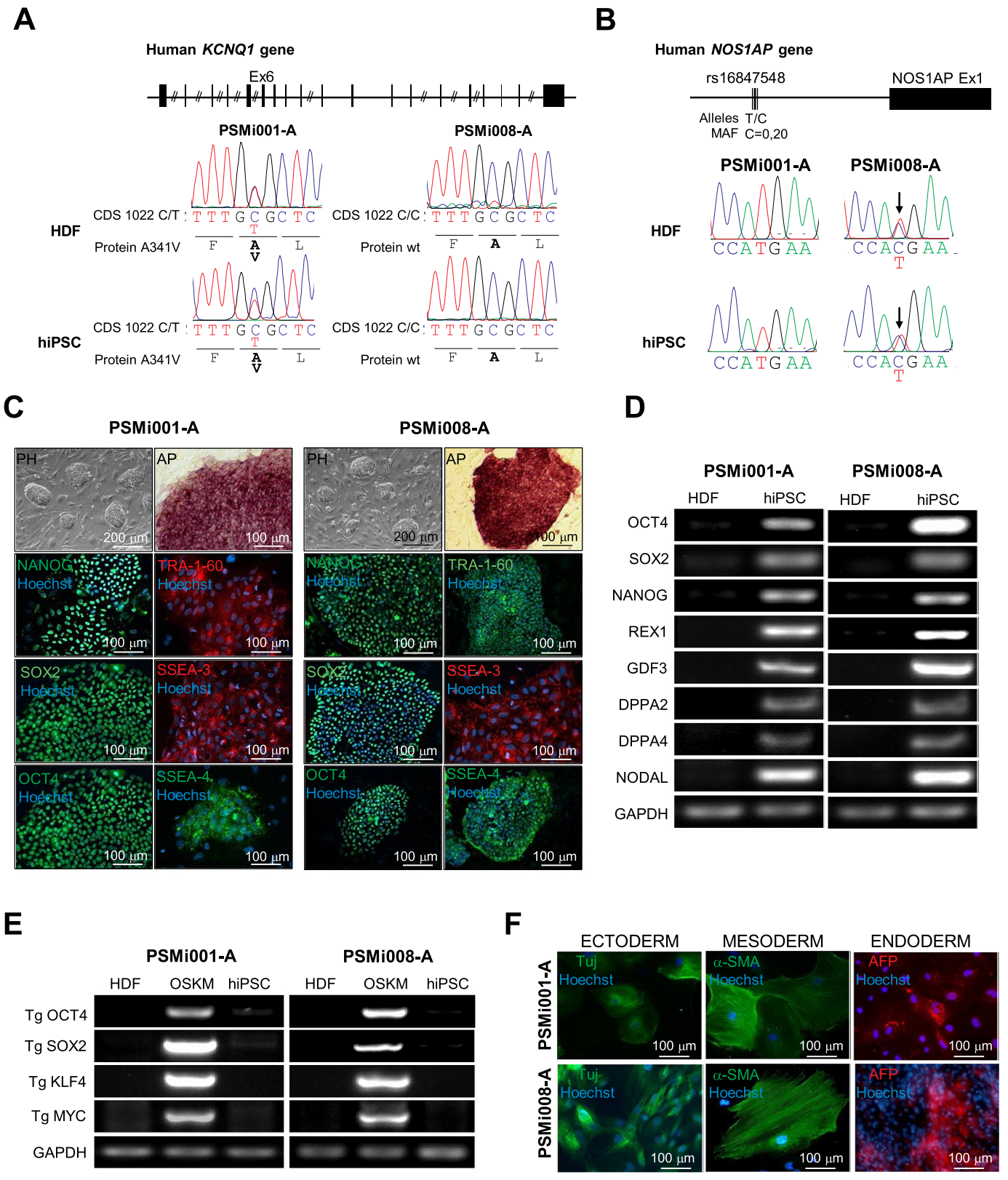

(caption on next page)

Fig. 1. Characterization of the PSMi001-A and PSMi008-A cell lines. A. Top: schematic representation of *KCNQ1* gene (exons are vertical lines/boxes). The *KCNQ1* coding sequence (CDS) used as a reference is the NCBI sequence NM_000218.2. Bottom: DNA sequencing results showing the mutation 1022 C/T in the *KCNQ1* exon 6 (Ex6) in heterozygosis in the PSMi001-A but not in PSMi008-A parental dermal fibroblasts (HDF) and hiPSC cell line (hiPSC). B. Top: schematic representation of NOS1AP gene upstream region. MAF is the minor allele frequency in the SA founder population. Bottom: DNA sequencing results showing the rs16847548 minor allele in heterozygosis in the PSMi008-A but not PSMi001-A parental dermal fibroblasts (HDF) and hiPSC cell line (hiPSC). C. PH: phase contrast images showing PSMi001-A and PSMi008-A morphology. AP: alkaline phosphatase colorimetric staining. All the other panels: immunofluorescence stainings showing uniform expression of the indicated markers of pluripotency in the PSMi001-A and PSMi008-A. Nuclei were counterstained with Hoechst 33258 (Hoechst, blue). D. RT-PCR analysis showing expression of pluripotency markers in PSMi001-A and PSMi008-A (hiPSC) compared with parental fibroblasts (HDF). E. RT-PCR analysis showing no expression of the four viral transgenes (Tg) in naïve fibroblasts (HDF), expression of Tg OCT4, SOX2, KLF4 and cMYC five days after transduction (OSKM) and silencing of the four Tg in PSMi001-A and PSMi008-A at passages 5 and 6 respectively. F. Immunofluorescence staining for markers of the 3 germ layers in iPSC-derived EBs: neuronal class tubulin beta III (Tuj) for ectoderm, smooth muscle actin (SMA) for mesoderm, and alpha Fetoprotein (AFP) for endoderm.

monstrated that this *NOS1AP* variant is significantly associated with increased risk of life-threatening events in LQTS individuals of this SA population (Crotti et al., 2009); therefore we anticipate that the use of this cell line will help us to elucidate the molecular mechanism by which this *NOS1AP* variant worsen the clinical phenotype.

To generate the hiPSCs, dermal fibroblasts were reprogrammed by retroviral infection of OCT4, SOX2, KLF4 and c-MYC. The obtained clones were maintained on feeders. Both PSMi001-A hiPSC and the parental fibroblasts (HDF) present the disease causing mutation on the *KCNQ1* gene, as proved by DNA sequencing, whereas PSMi008-A HDF and hiPSC are wt (Fig. 1A. *The KCNQ1 coding sequence -CDS- used as a reference is the NCBI sequence NM_000218.2*). PSMi008-A HDF and hiPSC are heterozygous for the rs16847548 minor allele, whereas PSMi001-A HDF and hiPSC are homozygous for the major allele (Fig. 1B. *MAF = minor allele frequency in the SA founder population*).

Both fibroblasts and the derived PSMi001-A and PSMi008-A hiPSCs show an identical DNA profile at 7 polymorphic loci, as shown by Short tandem Repeat (STR) analysis (available with the authors). Moreover, the DNA karyotyping revealed normal karyotype (46, XX for PSMi001-A and 46, XY for PSMi008-A) (Suppl Fig. 1A). Both hiPSC lines display embryonic stem cell (ES)-like morphology (Fig. 1C), and uniformly express the human ES surface antigens Tumor Related Antigen-1-60 (TRA-1-60), Stage Specific Embryonic Antigen-3 and -4 (SSEA-3, SSEA-4), and show alkaline phosphatase (AP) activity (Fig. 1C). Likewise, they express the pluripotent markers NANOG, OCT4, SOX2 (Fig. 1C-D), REX1, GDF3, DPPA2, DPPA4 and NODAL (Fig. 1D) at percentages higher than 98% (see immunocytochemistry counting in Suppl Fig. 1B). RT-PCR analysis in Fig. 1E shows no expression of the four viral transgenes (Tg) in naïve fibroblasts (HDF), clear expression of Tg in fibroblasts five days after transduction (OSKM) and silencing of the four Tg in both PSMi001-A and PSM008-A at passage 5 and 6, respectively.

PSMi001-A and PSMi008-A spontaneously form embryoid bodies (EBs) able to differentiate into cells belonging to the three germ layers: endoderm (alpha-fetoprotein - AFP), mesoderm (alpha smooth muscle actin- αSMA) and ectoderm (tubulin beta III - Tuj) (Fig. 1F).

Finally, we excluded the presence of mycoplasma contamination in our PSMi001-A and PSMi008-A lines (Suppl Fig. 1C).

Table 1
Characterization and validation of PSMi001-A and PSMi008-A cell lines.

Classification	Test	Result	Data
Morphology	Photography	Normal	Fig. 1C
Phenotype	Qualitative analysis	Positive immunostaining for the pluripotency markers OCT4, NANOG, SOX2, TRA-1-60, SSEA-3, SSEA-4	Fig. 1 panel C
		Positive staining for the alkaline phosphatase	Fig. 1 panel C
		Expression of the pluripotency markers OCT3/4, SOX2, NANOG, REX1, GDF3, DPPA2, DPPA4, NODAL, measured by RT-PCR.	Fig. 1 panel D
	Quantitative analysis	Immunocytochemistry counting: 99,2% NANOG$^+$ PSMi001-A cells, 98,6% OCT4$^+$ PSMi008-A cells.	Suppl Fig. 1 panel B
Genotype	Karyotype (300 G-banding) and resolution	46XX for PSMi001-A and 46XY for PSMi008-A. Resolution 450–500	Suppl. Fig. 1 panel A
Identity	Microsatellite PCR (mPCR)	Not performed	Not available
	STR analysis	7 sites tested for iPSC, all sites matched with donor HDF STR profile	Available with authors
Mutation analysis	Sequencing	PSMi001-A is heterozygous for the mutation c. 1022C > T p.A341V on the KCNQ1 gene,and homozygous for the rs16847548 major allele T. PSMi008-A is wt for KCNQ1, and heterozygous for the rs16847548 minor allele C.	Fig. 1 panels A and B
Microbiology and virology	Mycoplasma	Mycoplasma testing by RT-PCR. Negative	Suppl. Fig. 1, panel C
Differentiation potential	Embryoid body formation	The EBs expressed neuronal class tubulin beta III (Tuj) (ectoderm), smooth muscle actin (SMA) (mesoderm), and alpha Fetoprotein (AFP) (endoderm).	Fig. 1 panel F
Donor screening	HIV 1 + 2 Hepatitis B, Hepatitis C	Not performed	Not available
Genotype additional info	Blood group genotyping	Not performed	Not available
	HLA tissue typing	Not performed	Not available

Materials and methods

Expanded methods are provided in the Supplemental Methods section.

hiPSC generation

Skin fibroblasts were reprogrammed using four retroviruses encoding OCT4, SOX2, KLF4 and c-MYC. Emerging iPSC clones were manually picked, individually placed into a separate cell culture well and expanded on a feeder-layer of mitotically-inactivated mouse embryonic fibroblasts (iMEF), and grown in DMEM/F12 supplemented with 20% Knockout Serum Replacement (KO-SR), 2 mM L-glutamine, 50 U/ml penicillin, 50 U/ml streptomycin, 1% Non-Essential Amino Acids (NEAA), 0.1 mM beta-mercaptoethanol, 10 ng/ml basic Fibroblast Growth Factor (bFGF) (Table 1).

Mutation analysis

Genomic DNA was extracted with QIAamp DNA Blood Mini kit (Qiagen), and amplified with Phire Green Hot Start II PCR Master Mix (ThermoFisher) (see Table 2 for primer sequences and product size).

Table 2
Reagents details.

Antibodies used for immunocytochemistry			
	Antibody	Dilution	Company Cat # and RRID
Pluripotency markers	Rabbit anti Nanog	1:200	Stemgent *Cat#* 09–0020, *RRID:* AB_2298294
	Mouse anti Oct3/4 (C-10)	1:500	SCBT *Cat#* sc-5279, *RRID:* AB_628051
	Mouse anti Sox2	1:500	R&D Systems *Cat#* MAB2018, *RRID:* AB_358009
	Mouse anti TRA-1-60	1:100	Stemgent *Cat#* 09–0010, *RRID:* AB_1512170
	Rat anti SSEA-3	1:100	Millipore *Cat#* MAB4303, *RRID:* AB_177628
	Mouse anti SSEA-4	1:100	Stemgent *Cat#* 09–0006, *RRID:* AB_1512169
Differentiation markers (EBs)	Mouse anti neuronal class tubulin beta III (Tuj)	1:500	Covance *Cat#* MMS-435P, *RRID:* AB_2313773
	Mouse anti alpha smooth muscle actin (α-SMA)	1:1000	Millipore *Cat#* CBL171, *RRID:* AB_2223166
	Mouse anti alpha-fetoprotein (AFP)	1:500	Millipore *Cat#* SCR030, *RRID:* AB_597591
Secondary antibodies	Alexa-Fluor® 488 Goat anti-rabbit IgG	1:500	ThermoFisher Cat# A11008, *RRID:*AB_143165
	Alexa-Fluor® 594 Goat anti-rat IgM	1:500	ThermoFisher Cat# A21213, *RRID*: AB_11180463
	Alexa-Fluor® 488 Goat anti-mouse IgG	1:500	ThermoFisher Cat# A11001, *RRID*: AB_2534069
	Alexa-Fluor® 546 Goat anti-mouse IgG	1:500	ThermoFisher Cat# A11003, *RRID*: AB_141370
Primers			
	Target	Forward/reverse primer (5′-3′)	
Targeted mutation analysis/sequencing	KCNQ1 Exon 6	Fw: 5′- tggctgaccactgtccctct −3’	
	195 bp	Rev.: 5′- ccccaggaccccagctgtccaa −3’	
	rs16847548	Fw: 5’- aggggaacttaaaccgtgcc −3’	
	579 bp	Rev.: 5′- agcgccctctatcaccaatg −3’	
Pluripotency Markers (RT-PCR)	OCT4	Fw: 5’-gtactcctcggtccctttcc-3’	
	168 bp	Rev.: 5′-caaaaaccctggcacaaact-3’	
	SOX2	Fw: 5’-acaccaatcccatccacact-3’	
	273 bp	Rev.: 5′-tttttcgtcgcttggagact-3’	
	NANOG	Fw: 5’-ttccttcctccatggatctg-3’	
	213 bp	Rev.: 5′-tctgctggaggctgaggtat-3’	
	REX1	Fw: 5’-cagatcctaaacagctcgcagaat-3’	
	306 bp	Rev.: 5′-gcgtacgcaaattaaagtccaga-3’	
	GDF3	Fw: 5’-cttatgctacgtaaaggagctggg-3’	
	631 bp	Rev.: 5′-gtgccaacccaggtcccggaagtt-3’	
	DPPA4	Fw: 5’-ggagccgcctgccctggaaaattc-3’	
	408 bp	Rev.: 5′-tttttcctgatattctattcccat-3’	
	DPPA2	Fw: 5’-ccgtccccgcaatctccttccatc-3’	
	606 bp	Rev.: 5′-atgatgccaacatggctcccggtg-3’	
	NODAL	Fw: 5’-gggcaagaggcaccgtcgacatca-3’	
	234 bp	Rev.:5′-gggactcggtggggctggtaacgtttc-3’	
House-Keeping Genes (RT-PCR)	GAPDH	Fw 5’-catgttccaatatgattccaccc-3’	
	112 bp	Rev. 5′-gggatctcgctcctggaagat-3’	
Retroviral transgenes	Oct4 cDNA on pMXs-hOCT3/4	Fw: 5′-ccccagggccccattttggtacc-3’	
	339 bp		
	Sox2 cDNA on pMXs-hSOX-2	Fw: 5′-ggcacccctggcatggctcttggctc-3’	
	496 bp		
	cMyc cDNA on pMXs-hcMYC	Fw: 5′-caacaaccgaaaatgcaccagccccag-3’	
	542 bp		
	Klf4 cDNA on pMXs-hKLF4	Fw: 5′-acgatcgtggccccggaaaaggacc-3’	
	518 bp		
	pMX viral vector	Rev: 5′-ccctttttctggagactaaataaa-3’	

The resulting amplicons were purified and sequenced (Lightrun service - GATC Biotech AG – Germany).

STR analysis

STR analysis was carried out using PowerPlex® CS7 System kit (Promega), following the manufacturer's protocol. Fragments were run on a 3130xl capillary sequencer (Applied Biosystems). Genotypes were assigned using GeneMarker software (SoftGenetics).

Karyotyping

hiPSCs were blocked at metaphase by exposure to 10 µg/ml demecolcine solution (Sigma Aldrich) for 3 h. Karyotyping was performed using 300 G-banding chromosome analysis.

Immunocytochemistry

hiPSCs and their derivatives were grown on glass coverslips, and then fixed for 15 min in 4% paraformaldehyde (Affymetrix USB), permeabilized with 0.1% Triton X-100 (Sigma Aldrich) for 5 min, and blocked in 1% bovine serum albumin (BSA, Sigma Aldrich) for 1 h at room temperature (RT). Then they were incubated at RT with the primary antibody (Table 2) diluted in blocking solution for 1 h, washed three times, and incubated for 1 h at RT with an appropriate secondary antibody (Table 2). Finally, the cells were stained with 1 µg/ml of Hoechst 33258 (Sigma Aldrich). Images were acquired using the Carl Zeiss fluorescence microscope Observer.Z1 equipped with the Apotome system and AxioVision 6.0 software (Zeiss GmbH, Gottingen, Germany).

Immunocytochemistry counting

$NANOG^+$ and $OCT4^+$ cells were counted using the AxioVision 6.0 software (Zeiss GmbH, Gottingen, Germany). The total number of cells in each field was quantified by counting the nuclei stained with Hoechst 33258.

AP assay

AP was detected by using the Alkaline Phosphatase Staining kit II (00–0055 Stemgent).

RT-PCR

Total RNA was purified using TRIzol (ThermoFisher Scientific). cDNA was synthesized using the Superscript IV Reverse Transcriptase (ThermoFisher). RT-PCR was performed with the Phire Green Hot Start II PCR Master Mix (Thermo Scientific) and primers in Table 2.

EB formation

hiPSCs were enzimatically detached and grown for 7 days in non-adherent conditions in a modified iPS medium deprived of bFGF and containing 20% FBS instead of KO-SR. Forming EBs were then transferred to gelatin-coated dishes to allow differentiation in adhesion in the same medium for additional 7 days. Finally, the cells were processed for immunostaining of the three germ layers as described above.

Mycoplasma test

For the detection of mycoplasma in cell culture we used the EZ-PCR Mycoplasma Test Kit (Biological Industries).

Key resources table

Unique stem cell lines identifier	PSMi001-A PSMi008-A
Alternative names of stem cell lines	SA6.27-iPS SA2.3-iPS
Institution	Fondazione IRCCS Policlinico San Matteo, Pavia, Italy
Contact information of distributor	Massimiliano Gnecchi, m.gnecchi@unipv.it
Type of cell lines	hiPSC
Origin	human
Cell source	Dermal fibroblasts
Clonality	Clonal
Method of reprogramming	Retroviruses encoding for the human cDNA of OCT4, SOX2, cMYC, KLF4
Multiline rationale	Control and disease pair
Genetic modification	Yes
Type of modification	PSMi001-A: congenital mutation PSMi008-A:congenital single nucleotide polymorphism (SNP)
Associated disease	Long QT Syndrome type 1 (OMIM #192500)
Gene/locus	PSMi001-A: 1022C > T mutation on *KCNQ1* (NM_000218.2), 11p15.5-p15.4 PSMi008-A: rs16847548 variant (CM000663.2:g.162065484 T > C)
Method of modification	N/A
Name of transgene or resistance	N/A
Inducible/Constitutive system	N/A
Date archived/stock date	PSMi001-A: 30/12/2015 PSMi008-A: 25/2/2016
Cell line repository/bank	https://hpscreg.eu/cell-line/PSMi001-A https://hpscreg.eu/cell-line/PSMi008-A
Ethical approval	The study has been approved by the Ethics Committee of the University of Stellenbosch, South Africa, on the 4 March 2013, protocol number N13/01/002. We obtained patient written informed consent for both skin biopsy procedure and conservation of biological samples.

Acknowledgements

This work was supported by the Leducq Foundation for Cardiovascular Research [18CVD05] 'Towards Precision Medicine with Human iPSCs for Cardiac Channelopathies', by the Italian Ministry of Health, "Ricerca Corrente" projects numbers 08064017 and 08064018, and by a grant to the Department of Molecular Medicine of the University of Pavia under the initiative "Dipartimenti di Eccellenza" (2018–2022).

Appendix A. Supplementary data

Supplementary data to this article can be found online at https://doi.org/10.1016/j.scr.2019.101510.

References

Brink, P.A., Crotti, L., Corfield, V., Goosen, A., Durrheim, G., Hedley, P., Heradien, M., Geldenhuys, G., Vanoli, E., Bacchini, S., Spazzolini, C., Lundquist, A.L., Roden, D.M., Jr, A.l. George, Schwartz, P.J., 2005. Phenotypic variability and unusual clinical severity of congenital long-QT syndrome in a founder population. Circulation. 112, 2602–2610.

Crotti, L., Monti, M.C., Insolia, R., Peljto, A., Goosen, A., Brink, P.A., Greenberg, D.A., Schwartz, P.J., George Jr., A.L., 2009. NOS1AP is a genetic modifier of the long-QT syndrome. Circulation 120, 1657–1663.

Gnecchi, M., Stefanello, M., Mura, M., 2017. Induced pluripotent stem cell technology: toward the future of cardiac arrhythmias. Int. J. Cardiol. 237, 49–52.

Mehta, A., Ramachandra, C.J.A., Singh, P., Chitre, A., Lua, C.H., Mura, M., Crotti, L., Wong, P., Schwartz, P.J., Gnecchi, M., Shim, W., 2018. Identification of a targeted and testable antiarrhythmic therapy for long-QT syndrome type 2 using a patient-specific cellular model. Eur. Heart J. 39, 1446–1455.

Schwartz, P.J., PJ, Gnecchi M., Dagradi, F., Castelletti, S., Parati, G., Spazzolini, C., Sala, L., Crotti, L., 2019. From patient-specific induced pluripotent stem cells to clinical translation in long QT syndrome type 2. Eur. Heart J. https://doi.org/10.1093/eurheartj/ehz023. Feb 6. (Epub ahead of print).